

Impurity-induced modes of Mg, As, Si, and C in hexagonal and cubic GaN

G. Kaczmarczyk, A. Kaschner, A. Hoffmann, and C. Thomsen

Institut für Festkörperphysik, Technische Universität Berlin, Hardenbergstrasse 36, 10623 Berlin, Germany

(Received 26 March 1999)

We present a cluster-model calculation of local vibrational modes in hexagonal GaN using the valence-force model of Keating and Kane with valence-force parameters fitted to Raman and neutron-scattering experiments. We used the scaling-factor approximation to describe the interatomic forces of the central defect atom. For hexagonal GaN:Mg we find three modes at 136, 262, and 656 cm^{-1} in good agreement with experiments. For cubic GaN:As the isolated impurity atom gives us local modes at 95, 125, 151, and 250 cm^{-1} , which were observed as sharp lines in the experiment. For Si and C defects, for which local modes have not yet been reported, a similar choice of scaling factor as for Mg and As leads to modes that strongly hybridize with the host phonons.

I. INTRODUCTION

GaN has become the focus of wide band-gap semiconductor research.¹ In order to use GaN in device applications it has to be doped; while n doping is readily achieved successful p doping has been reported only with Mg. The dopant atoms, apart from changing the electrical properties of a material, can also appear in the vibrational spectrum of the host. Depending on the mass and also the bonding forces of the dopant atoms there may be localized vibrational modes in the phonon spectrum as observed by optical or neutron spectroscopy. In general, two types of local vibrations may be distinguished: local modes and resonance modes. A local mode is characterized by its frequency, which lies in the range forbidden for the modes of the perfect host crystal. Its vibration amplitude is large at the impurity site and decreases rapidly with increasing distance from the impurity. The frequency of the resonance modes lies in the range of frequencies allowed to the modes of the perfect host crystal. Its vibration amplitude is significant not only directly at the impurity atoms but also for the neighboring atoms. In case of a large phonon density of states such modes hybridize strongly and are difficult to observe experimentally. In practice, if observed, the frequency of a local mode may be used to determine the type of adatom and its relative strength the concentration.^{2,3}

Theoretically, local vibrational modes may be described by a variety of methods. Early calculations of the impurity-induced vibrations were based on Green's-function theory in the form of the one-parameter defect model of Grimm *et al.*⁴ Their approach was the method of choice for a large variety of impurities in numerous zinc-blende-type crystals.⁵⁻⁷ The newer calculations of elastic properties governing the lattice vibrations use a supercell method together with frozen-phonon model (e.g., Refs. 8-11). This method was used to calculate the forces only for a special and simple atomic displacement and not applied to calculations of localized vibrations. Another method uses first-principles calculations of the interatomic forces for simple displacements of the nearest neighbors of the defect to determine the parameters of a valence-force model.^{12,13} In a second step, these parameters are used to calculate the phonon dispersion curves and den-

sity of phonon states. With this method the local vibrational modes at several impurities in III-V compounds were calculated.¹³⁻¹⁶ *Ab initio* results for the phonon frequencies or for the local modes in hexagonal GaN have not yet become available.

II. MODEL

In this paper, we focus on the local vibrations of Mg, As, Si, and C impurities in hexagonal GaN and of an As impurity in cubic GaN. Our model is based on the harmonic approximation of forces between atoms and a modified valence-force model of Keating and Kane. The simple model of Keating¹⁷ for bond stretching and bond bending forces was extended by Kane¹⁸ to include up to the third-nearest neighbor interactions as well as Coulomb interaction. Their model was originally developed for cubic crystals in which case there are eight independent parameters and an effective charge for the long-range Coulomb interaction. For hexagonal symmetry the valence-force model was generalized by Göbel *et al.*¹⁹ The anisotropy of hexagonal GaN was taken into account by introducing two sets of parameters: one describing interactions along the c axis and one for interactions perpendicular to the c axis. They were used to set up the dynamical matrix, the eigenvalues of which are the squares of vibrational frequencies, and the Kane parameters were obtained for the perfect crystal from a calculation of the phonon dispersions curves and a comparison with second-order Raman spectra and neutron spectra of hexagonal GaN.

In crystals vibrational modes may be localized around a defect because of the difference in mass of the defect compared to the host atom or the change in electron density resulting in changes of the interatomic forces in the vicinity of the defect. In order to determine the eigen-frequencies and -vectors (and hence symmetry) of a localized vibration we constructed a cluster of host material around the defect and adopted the scaling-factor approximation²⁰ to describe the changes in the interatomic forces near the defect. The cluster contained 296 vibrating atoms arranged in 34 so-called coordination shells. The first shell is the central atom of the cluster, i.e., the impurity itself. The remaining shells are ordered by the distance of the shell atoms to the central atom,

i.e., the second shell consists of the ligand atom in the c -axis direction and the third shell represents the three ligands of the off-axis direction. In case of magnesium the impurity replaces a Ga atom of the perfect host crystal, and the second and third shells contain the four nitrogen atoms as nearest neighbors of a Ga site. To calculate the phonon density of states, the Brillouin zone was divided into a $100 \times 100 \times 100$ mesh. The identification of the symmetry of the calculated modes occurred by the application of symmetry-adapted functions.

The scaling-factor approximation assumes an equal relative change of all parameters in the vicinity of the impurity. If p is a parameter of the perfect crystal, the corresponding value at the defect site is modified by the factor $(1+s)$. The scaling factor s is thus a measure of change of the interatomic forces at the impurity. A negative s indicates a local softening of the interatomic forces and a positive s means that the defect site is more strongly bound to its nearest neighbors than the atoms of the perfect crystal. From the calculations, we obtain the energy and localization of the modes as a function of scaling factor s . Comparing with the experimental values, we were able to determine the specific scaling factor for the impurities considered.

In determining the localized vibrational modes we proceeded as follows. In a first step we determined the valence-force parameters of Kane for the perfect hexagonal GaN crystal. Because the full dispersion curves from neutron scattering are not yet available we compared the calculation with the zone-center frequencies observed in Raman scattering. In this procedure the upper B_1 silent mode remained unconsidered during fitting. In order to include experimental data for points away from Γ we compared the calculated phonon density of states of hexagonal GaN with experimental data available from second-order Raman spectra.²¹ Recently, Nipko *et al.*²² presented the neutron density of states of hexagonal GaN. A comparison between the calculated density of states of Ref. 21 showed good agreement in the energy range up to 600 cm^{-1} (75 meV). Slight differences were found in the high-frequency range. In order to improve our dispersion curves, we shifted the so far undetermined upper B_1 silent mode at Γ (from 642 to 706 cm^{-1}) and K (from 616 to 632 cm^{-1}) and the optical branch (from 576 to 617 cm^{-1}) at the K point of the Brillouin zone. These additional constraints resulted in an excellent agreement with the neutron and Raman density of states; in particular they resulted in a minimum in the phonon density of states at about 81 meV as observed in Ref. 22. Figure 1(a) shows the improved calculated phonon-dispersion curves of hexagonal GaN and Fig. 1(b) the corresponding density of phonon states together with the neutron experiments. Our calculations of the local modes are based on these dispersion curves.

III. RESULTS

A. Mg in α -GaN

We turn now to the local vibrational modes in hexagonal GaN. Figure 2 shows the first-order Raman spectra of Mg-doped GaN taken from Ref. 23. In addition to the phonons of the perfect crystal [$A_1(\text{TO})$ at 533 cm^{-1} , E_2 at 568 cm^{-1} and $A_1(\text{LO})$ at 735 cm^{-1}], five Mg-concentration depended modes at 136 , 262 , 320 , 595 , and 656 cm^{-1} and not present

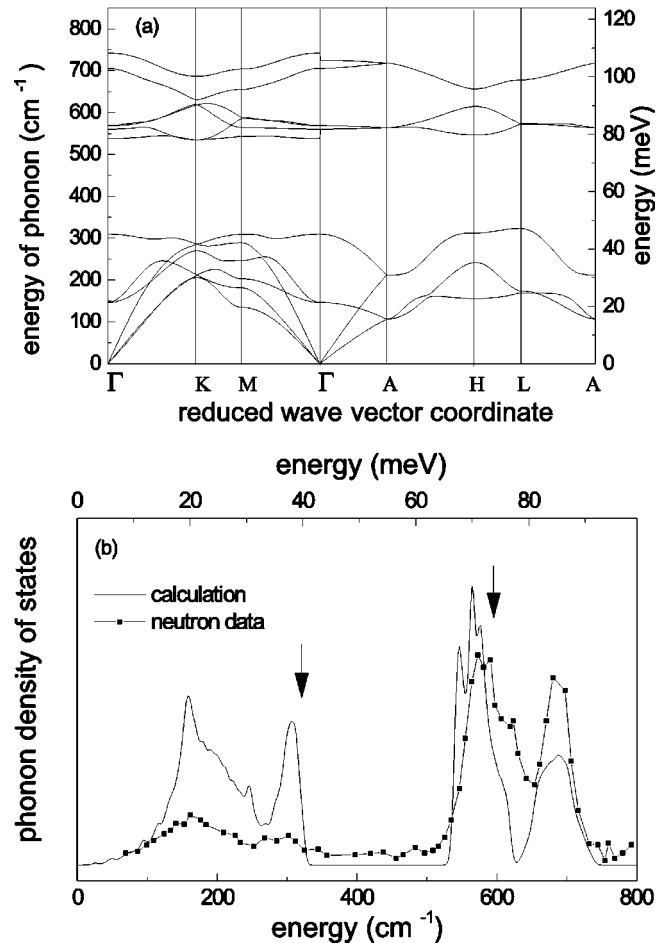


FIG. 1. (a) Calculated phonon dispersion curves of hexagonal GaN. (b) Comparison of the calculated phonon density of states (PDOS) and the experimental neutron values of hexagonal GaN. The arrows mark the disorder-activated modes at 320 and 595 cm^{-1} . Experimental data taken from Ref. 22.

in pure GaN were observed; all these modes exhibited A_1 symmetry.²³ The modes at 136 , 262 , and 656 cm^{-1} are located in energy ranges with low density of phonon states in the perfect crystal (Fig. 1) and were assigned to local vibrational modes of magnesium in GaN. The peaks at 320 and 595 cm^{-1} are in an energy range with a high density of phonon states for the perfect crystal.²⁴ These vibrations were assigned to disorder-activated scattering, in which built-in defects, due the loss of translational symmetry, yield a relaxation of the $\vec{q}=0$ section rule for first-order Raman scattering. Similar observations in the Raman spectra at 300 cm^{-1} were reported by Ref. 25, who interpreted this additional mode as resulting from damage of the crystal lattice induced by the post-growth ion implantation.

In order to verify these assignments we carried out calculations within the above model. Figure 3 shows the dependence of the energy of the local modes on scaling factor for the Mg defect in hexagonal GaN. Several local vibrational modes were found both in the range forbidden for the modes of the perfect host crystal, the so-called phonon gap between ~ 340 and $\sim 540 \text{ cm}^{-1}$, and in the region of the host's acoustical and optical modes (below 330 cm^{-1} and between 540 and 760 cm^{-1} , respectively). We identified a local vibrational mode by the condition that the sum of the ampli-

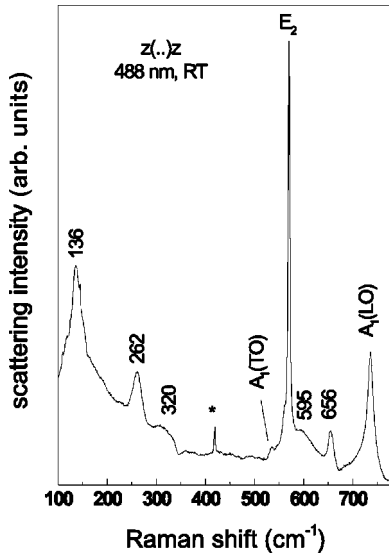


FIG. 2. Room-temperature Raman spectrum of Mg-doped GaN in the low-energy range. The spectrum was recorded in backscattering geometry with the 488-nm line of an Ar⁺/Kr⁺ mixed-gas laser as excitation. In addition to the host modes five modes are observed at the indicated frequencies. The peak marked by an asterisk is a phonon from the substrate. (from Ref. 23).

tudes of the eigenvector of all atoms in the first three shells around the defect is larger than about 20% of the vibration amplitude of the entire cluster. The circles in Fig. 3 describe local phonons with A_1 symmetry, the squares phonons with E symmetry. The best agreement with the experimental values (136, 262, and 656 cm⁻¹, open symbols) is achieved for a scaling factor of $s = -0.15$; this implies that the force constants in the vicinity of the Mg defect are about 15% weaker than those of the perfect crystal. The energies of these vibrations are located in the region of the host phonons and the vibrations, due to a hybridization with the host phonons, are not strictly limited to the impurity and the nearest neighbor.

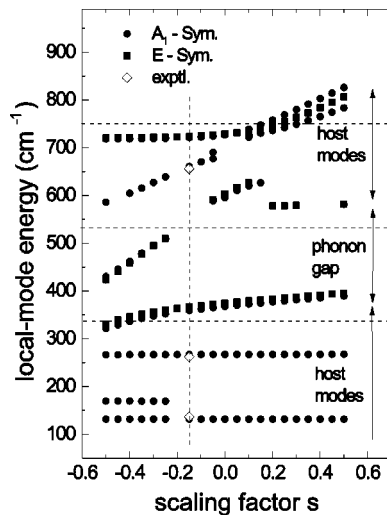


FIG. 3. Local vibrational-mode frequencies of magnesium as a function of scaling factor. The solid symbols represent the calculated A_1 and E modes with a localization of over 20% and the A_1 modes at about 266 cm⁻¹ with a slightly smaller localization (17%) on the first three shells. The open symbols are experimental values.

TABLE I. Summary of the calculated local vibrational modes of GaN:Mg and GaN:As in comparison with the experimental values. The symmetries of the modes are given in parentheses. (s) describes sharp lines assigned to isolated As impurities and (b) broad, presumably cluster-related excitations. Experimental values taken from Refs. 23 and 27.

GaN:Mg		GaN:As		
hexagonal	cubic	hexagonal		
exp. cal.	exp. calc.	exp. calc.		
($s = -0.15$)	($s = -0.2$)	($s = -0.2$)		
136	132 (A_1)	95 (s)	92 (T_2)	96
262	267 (A_1)	102.5		
	359 (A_1)	125 (s)	126 (T_2)	118 (A_1)
	366 (E)	150 (s)	146 (A_1)	
656	660 (A_1)	190 (b)		178 185 (A_1)
	721 (A_1)	220 (s)		
	724 (E)	235 (b)		235 239 (A_1)
		250 (s)	257 (T_2)	

In Table I we compare the calculated vibrational frequencies of the Mg impurity in hexagonal GaN with the experiment. In addition to the vibrations described above, we found modes around 320, 360, 596, and 720 cm⁻¹ with a localization of over 20% in the calculation. However, the modes around 320 and 595 cm⁻¹ are also present in the perfect crystal and correspond to energies with a large density of states [see Fig. 1(b)]. This confirms the assignment of these modes to disorder-activated scattering.^{23,25} The calculated modes around 360 cm⁻¹ are not observed in experiments. The modes around 720 cm⁻¹ are located in the range of A_1 (LO) phonon. The energetic position of these local modes could explain the observed asymmetry of the A_1 (LO) phonon (see Fig. 2).

B. As in α - and β -GaN

Another technologically interesting impurity in GaN is As, as in the growth of *cubic* GaN on a GaAs substrate, some As atoms may diffuse from the substrate into the GaN layer. It was shown that in low-temperature Raman spectra of GaN films grown epitaxially on GaAs contain, in addition to the host phonons, a series of sharp lines in the energy range from 95 to 250 cm⁻¹.^{26,27} Ramsteiner *et al.*²⁶ found peaks at 151 cm⁻¹ (18.7 meV) and 217 cm⁻¹ (26.9 meV) and attributed them to excitations in hexagonal GaN and peaks at 189 cm⁻¹ (23.4 meV) and 237 cm⁻¹ (29.4 meV) which were claimed to originate from cubic GaN. They interpreted these excitations as electronic Raman transitions in a shallow donor. Over 10 lines, the most intense ones located at 95, 125, 150, 190, 220, 235, and 250 cm⁻¹ were found by Siegle *et al.*²⁷ They showed from magnetic field and pressure dependence that all lines should rather be of vibrational and not of electronic origin. A comparison of several series of samples showed that the lines occurred only in samples grown on GaAs substrates and in As doped GaN layers on sapphire. This suggested strongly that these lines are associated with As impurities. The lines at 190 and 235 cm⁻¹ were attributed to a defect cluster based on their large halfwidth.

In order to verify this interpretation we investigated the possibility that local vibrations of the As impurities in cubic or hexagonal GaN layer are the origin for the observed Raman lines. We carried out calculations within the described cluster model for As impurities in both structural modifications of GaN. The valence-force parameters of Kane in cubic GaN were determined similarly by a fit to the phonon dispersion curves of the perfect GaN crystal. For the fit we used the experimental Raman frequencies at the Γ point.²¹ The calculations of the local vibrational modes in cubic GaN were performed using a cluster of 281 vibrating atoms arranged in 17 coordination shells, embedded in the nonvibrating crystal.

For the identification of the local vibrational modes in hexagonal case we used a similar condition as before, i.e., that the sum of the amplitudes of the eigenvector of all atoms in the first three shells around the defect is larger than about 25% of the vibrational amplitude of the entire cluster. The best agreement with the experimental values (95, 125, 150, and 250 cm^{-1}) is achieved for a scaling factor $s \approx -0.15 \pm 0.05$ in cubic GaN. The remaining experimental modes at 190, 220, and 235 cm^{-1} were not found in the cubic modification. The localized modes between 550 and 740 cm^{-1} are located in the range of the host phonons of cubic GaN; they are hence difficult to observe and not listed in Table I. The similarity in the scaling factors of Mg and As is somewhat surprising since As is an isoelectronic impurity and Coulomb effects should be much smaller than for the donor Mg.

The local modes of As impurities in *hexagonal* GaN at 96, 178, and 235 cm^{-1} were reported by Ref. 27. We obtain good agreement between the experimental values and the calculated local modes (at 118, 185, 239 cm^{-1}) for the same scaling factor $s \approx -0.15 \pm 0.05$. The energies of the vibrations at 185 and 239 cm^{-1} coincide with experimental values of the broad excitations in cubic GaN. Our calculation thus suggests that while the origin of the modes at 95, 125, 150, and 250 cm^{-1} is an *isolated* As impurity in *cubic* GaN, the broad modes at 190 and 235 cm^{-1} in nominally cubic GaN result from other more complicated forms of As incorporation or an As impurity incorporated in the hexagonal modification. In Table I we compare the calculated vibrational frequencies of the As impurity in cubic and hexagonal GaN with the experiment.

C. Si, C in α -GaN

Other dopants of interest for GaN are Si and C.^{28–30} To our knowledge, vibrational modes for Si- or C-doped GaN have not been reported so far; we describe here our results on GaN:Si and GaN:C.

The slight mass difference of both impurities (Si-28 vs Mg-24) explains the similar behavior of the local modes. Our Raman studies of Si-doped GaN samples showed no experimental evidence of the local vibrations up to a concentration of 10^{20} cm^{-3} for Si. The absence of the local modes in the Raman spectra may be explained either in terms of a much reduced Raman cross section or due their strong hybridization with the host phonons. Comparing the signal amplitude at equal concentration levels, the cross section of a vibration localized at a Si defect would have to be 100 times lower than that of Mg. Alternatively, the experimental observation

of these modes may be prevented by a strong hybridization with the host modes, which occurs for a scaling factor in the range $-0.2 < s < 0.2$. This range is reasonable for s ; earlier calculations of local modes in GaN $s = -0.1$ was used for the Ti- and $s = 0.175$ for the Fe defect.¹⁹ Furthermore, it is known that donors like Si or C in GaAs or GaP have a strengthened bond compared to the pure crystal.¹³ Therefore, we believe that s should be positive also for Si and C in GaN. Strong hybridization is thus a possible reason for the local modes of Si to be so weak that they have not yet been observed in GaN. For a scaling factor between 0 and 0.2, we found three frequencies with E and five with A_1 symmetry. The energies are 310 \pm 2 cm^{-1} (A_1), 359 \pm 4 cm^{-1} (A_1), 364 \pm 4 cm^{-1} (E), 613 \pm 18 cm^{-1} (A_1), 613 \pm 13 cm^{-1} (A_1), 615 \pm 14 cm^{-1} (E), 727 \pm 5 cm^{-1} (A_1), and 730 \pm 8 cm^{-1} (E). The error given describes the energetic variation of the local mode for the scaling-factor range $0 \leq s \leq 0.2$.

In contrast to the Mg and Si impurities carbon atoms are imbedded on the N-lattice site.³¹ The small mass difference between C- and N-atoms causes C-induced modes with frequencies close to those of phonons of the perfect host crystal. Choosing the same range of scaling factor the energy of these resonance modes are 601 \pm 8 cm^{-1} (E), 606 \pm 10 cm^{-1} (A_1), 678 \pm 2 cm^{-1} (E), 715 \pm 3 cm^{-1} (E), 744 \pm 17 cm^{-1} (A_1), and 747 \pm 20 cm^{-1} (E). Similarly to the situation in GaN:Si, we did not observe local modes experimentally in C-doped samples (up to a concentration of 10^{21} cm^{-3}); the calculated frequencies lie in the range of high phonon density of the host making them too weak to be observed (see also Fig. 1). No modes are expected in the phonon gap region or above the optical phonons for this range of s .

IV. SUMMARY

In summary, local vibrational modes of Mg, As, Si, and C impurities have been investigated using a modified valence-force model of Keating and Kane. Our model verifies the origin of the modes at 136, 262, and 656 cm^{-1} as vibrations of the Mg impurity in GaN. Our calculations for the GaN:As system confirmed that most of the sharp excitations observed at low temperature can be attributed to local modes of As impurity in cubic GaN. The broad modes are more likely to originate from As-complexes or from hexagonal GaN:As regions incorporated into the cubic GaN. For Mg and As we found scaling factors that indicated a weakening of the bonds compared to their value in the pure crystal. For the isoelectronic impurity As the softening is smaller ($s \approx -0.15$) than for the acceptor Mg ($s = -0.2$). This result is consistent with the finding of Newman for acceptors in GaAs and GaP.¹³

The calculated energies of almost all local modes are in good agreement with the results obtained by Raman spectroscopy. We predicted possible frequencies for the local vibrational modes in Si- and C-doped GaN crystals and showed that for our choice of scaling factor a strong hybridization with host phonons is expected and is hence the likely reason for not observing the vibration of these impurities in GaN.

- ¹*Physics and Applications of Group III-Nitride Semiconductor Compounds*, edited by B. Gil (Oxford University Press, Oxford, 1997).
- ²R. Murray, R. C. Newman, M. J. L. Sangster, R. B. Beall, J. J. Harris, P. J. Wright, J. Wagner, and M. Ramsteiner, *J. Appl. Phys.* **66**, 2589 (1989).
- ³J. Wagner, M. Maier, R. Murray, R. C. Newman, R. B. Beall, and J. J. Harris, *J. Appl. Phys.* **69**, 971 (1991).
- ⁴A. Grimm, A. A. Maradudin, I. P. Ipatova, and A. V. Subashiev, *J. Phys. Chem. Solids* **33**, 775 (1972).
- ⁵M. Zigone, M. Vandevyver, and D. N. Talwar, *Phys. Rev. B* **24**, 5763 (1981).
- ⁶D. N. Talwar and Bal K. Agrawal, *Phys. Rev. B* **9**, 2539 (1974); **12**, 1432 (1975).
- ⁷P. Plumelle, D. N. Talwar, M. Vandevyver, K. Kunc, and M. Zigone, *Phys. Rev. B* **20**, 4199 (1979).
- ⁸H. Wendel and R. M. Martin, *Phys. Rev. B* **19**, 5251 (1979).
- ⁹M. T. Yin and M. L. Cohen, *Phys. Rev. Lett.* **45**, 1004 (1980); *Phys. Rev. B* **26**, 3259 (1982).
- ¹⁰K. Kunc and R. M. Martin, *Physica B* **117/118**, 511 (1983).
- ¹¹A. Baldereschi and R. Resta, in *Ab Initio Calculation of Phonon Spectra*, edited by J. T. Devreese, V. E. Van Doren, and P. E. Van Camp (Plenum Press, New York, 1983), Vol. 1.
- ¹²M. Scheffler and U. Scherz, *Mater. Sci. Forum* **10**, 353 (1986).
- ¹³R. C. Newman, E. G. Grosche, M. J. Ashwin, B. R. Davidson, D. A. Robbie, R. S. Leigh, and M. J. L. Sangster, *Mater. Sci. Forum* **258-263**, 1 (1997).
- ¹⁴U. Scherz and C. Schrepel, *Mater. Sci. Forum* **196-201**, 1571 (1995).
- ¹⁵K. Petzke, C. Göbel, C. Schrepel, P. Thurian, and U. Scherz, *Mater. Sci. Forum* **258-263**, 1179 (1997).
- ¹⁶K. Petzke, C. Schrepel, and U. Scherz, *Z. Phys. Chem. (Munich)* **201**, 317 (1997).
- ¹⁷P. N. Keating, *Phys. Rev.* **145**, 637 (1966).
- ¹⁸E. O. Kane, *Phys. Rev. B* **31**, 7865 (1985).
- ¹⁹C. Göbel, C. Schrepel, U. Scherz, P. Thurian, G. Kaczmarczyk, and A. Hoffmann, *Mater. Sci. Forum* **258-263**, 1173 (1997).
- ²⁰R. M. Feenstra, R. J. Hauenstein, and T. C. McGill, *Phys. Rev. B* **28**, 5793 (1983).
- ²¹H. Siegle, G. Kaczmarczyk, L. Filippidis, A. P. Litvinchuk, A. Hoffmann, and C. Thomsen, *Phys. Rev. B* **55**, 7000 (1997).
- ²²J. C. Nipko, C.-K. Loong, C. M. Balkas, and R. F. Davis, *Appl. Phys. Lett.* **73**, 34 (1998).
- ²³A. Kaschner, H. Siegle, G. Kaczmarczyk, M. Strassburg, A. Hoffmann, C. Thomsen, U. Birkle, S. Einfeld, and D. Hommel, *Appl. Phys. Lett.* **74**, 3281 (1999).
- ²⁴H. Harima, T. Inoue, Y. Sone, S. Nakashima, M. Ishida, and M. Taneya, *Phys. Status Solidi B* **216**, 789 (1999).
- ²⁵W. Limmer, W. Ritter, R. Sauer, B. Mensching, C. Liu, and B. Rauschenbach, *Appl. Phys. Lett.* **72**, 2589 (1998).
- ²⁶M. Ramsteiner, J. Menninger, O. Brandt, H. Yang, and K. H. Ploog, *Appl. Phys. Lett.* **69**, 1276 (1996).
- ²⁷H. Siegle, A. Kaschner, A. Hoffmann, I. Broser, C. Thomsen, S. Einfeldt, and D. Hommel, *Phys. Rev. B* **58**, 13 619 (1998).
- ²⁸P. Boguslawski and J. Bernholc, *Phys. Rev. B* **56**, 9496 (1997).
- ²⁹W. Kim, A. E. Botchkarev, A. Salvador, G. Popovici, H. Tang, and H. Morkoc, *J. Appl. Phys.* **82**, 219 (1997).
- ³⁰K. H. Ploog and O. Brandt, *J. Vac. Sci. Technol. A* **16**, 1609 (1998).
- ³¹J. Neugebauer and C. G. Van de Walle, *Festkörperprobleme* **35**, 25 (1996).